Phorbol Esters Induce Death in MCF-7 Breast Cancer Cells with Altered Expression of Protein Kinase C Isoforms

Role for p53-independent Induction of *gadd45* in Initiating Death

James E. de Vente,[§] Cynthia A. Kukoly,[*] Winifred O. Bryant,[*] Karla J. Posekany,[§] Jianming Chen,[*] Donald J. Fletcher,[‡] Peter J. Parker,[||] George J. Pettit,[¶] Guillermina Lozano,[**] Paul P. Cook,[*] and D. Kirk Ways[*§]

[*]Departments of Medicine, [‡]Anatomy/Cell Biology, and [§]Microbiology/Immunology, East Carolina University School of Medicine, Greenville, North Carolina 27858; [||]Imperial Cancer Research Fund, Protein Phosphorylation Laboratory, London, United Kingdom WC2A 3PX; [¶]Cancer Research Institute, Arizona State University, Tempe, Arizona 85287; and [**]Department of Molecular Genetics, M. D. Anderson Cancer Center, University of Texas, Houston, Texas 77030

Abstract

Protein kinase C (PKC) modulates growth, differentiation, and apoptosis in a cell-specific fashion. Overexpression of PKC-α in MCF-7 breast cancer cells (MCF-7-PKC-α cell) leads to expression of a more transformed phenotype. The response of MCF-7 and MCF-7-PKC-α cells to phorbol esters (TPA) was examined. TPA-treated MCF-7 cells demonstrated a modest cytostatic response associated with a G_1 arrest that was accompanied by Cip1 expression and retinoblastoma hypophosphorylation. While p53 was detected in MCF-7 cells, evidence for TPA-induced stimulation of p53 transcriptional activity was not evident. In contrast, TPA treatment induced death of MCF-7-PKC-α cells. Bryostatin 1, another PKC activator, exerted modest cytostatic effects on MCF-7 cells while producing a cytotoxic response at low doses in MCF-7-PKC-α cells that waned at higher concentrations. TPA-treated MCF-7-PKC-α cells accumulated in G_2/M, did not express p53, displayed decreased Cip1 expression, and demonstrated a reduction in retinoblastoma hypophosphorylation. TPA-treated MCF-7-PKC-α cells expressed *gadd45* which occurred before the onset of apoptosis. Thus, alterations in the PKC pathway can modulate the decision of a breast cancer cell to undergo death or differentiation. In addition, these data show that PKC activation can induce expression of *gadd45* in a p53-independent fashion. (*J. Clin. Invest.* 1995. 96:1874–1886.) Key words: protein kinase C • phorbol esters • breast cancer • apoptosis • p53

Introduction

The protein kinase C (PKC)[1] gene family lies on signal transduction pathways regulating growth and differentiation in a variety of cell types (1, 2). In addition, activation of this signaling pathway modulates induction of apoptosis in a cell-specific fashion. In certain cells, phorbol ester–stimulated activation of PKC inhibits apoptosis while in other cells a death program is initiated by activation of PKC (3–7). Beyond describing the ability of PKC to modulate apoptosis, little is known of the mechanisms either within the PKC pathway or signaling cascades distal to PKC that are responsible for producing these disparate, cell-specific responses. The existence of at least 12 members in the PKC gene family may, in part, serve as a mechanism responsible for the diverse responses elicited by activating this pathway (1, 2). Differences in substrate specificity, subcellular localization, and sensitivity to agonist-induced downregulation among the individual PKC isoforms may serve as possible mechanisms by which these varied cellular responses are elicited (1, 2). Thus, the array of isoforms expressed by a cell may determine its response to PKC activation. In addition to the array of isoforms initially expressed, cellular responses requiring chronic activation of the PKC pathway may also be influenced by the different sensitivities of individual isoforms to activation-induced proteolytic downregulation. Alternatively, differences in pathways activated by and distal to PKC that control growth, differentiation, and apoptosis could underlie the diversity of cellular responses to PKC activation.

A role for PKC in modulating growth of breast neoplasms has been suggested from various observations (8–15). To directly examine a role for PKC in altering the growth of breast cancer cells, we have generated a MCF-7 human breast cancer cell line that was stably transfected with and overexpresses PKC-α (MCF-7-PKC-α cells). In comparison to the parental MCF-7 cell, the MCF-7-PKC-α cell displays a more transformed, aggressive phenotype as evidenced by an increased proliferative rate, anchorage-independent growth, loss of an epithelioid appearance, downregulation of estrogen receptor expression, and enhanced tumorigenicity with metastatic potential in nude mice (16). These findings demonstrated that alterations in the PKC pathway are associated with significant changes in the proliferative capacity and differentiation status of breast cancer cells.

Given the significant phenotypic alterations observed in MCF-7-PKC-α cells, it was of interest to examine the response

This work was presented in abstract form at the 76th Annual Meeting of the Endocrine Society in Anaheim, CA, on 18 June 1994.

Address correspondence to D. Kirk Ways, M.D., Ph.D., East Carolina University School of Medicine, Department of Medicine, Greenville, NC 27858. Phone: 919-816-2567; FAX: 919-816-3096.

Received for publication 24 February 1995 and accepted in revised form 16 June 1995.

1. *Abbreviations used in this paper:* CAT, chloramphenicol acetyl transferase; Cip1, cyclin-dependent kinase interacting protein that has also been referred to as WAF1 and p21; MCF-7-PKC-α cells, MCF-7 cells that were stably transfected with and overexpress PKC-α; MG-15-CAT, a mutated, non–p53-responsive CAT construct; p0.5 CAT, a reporter construct controlled by −320/+210 of the p53 promoter; PG-13-CAT, a p53-responsive reporter plasmid; PKC, protein kinase C; Rb, retinoblastoma; TPA, tetradecanoyl phorbol-13-acetate.

J. Clin. Invest.

0021-9738/95/10/1874/13 $2.00
Volume 96, October 1995, 1874–1886

of this cell to phorbol ester–stimulated activation of PKCs. Parental MCF-7 cells treated with tetradecanoyl phorbol-13-acetate (TPA) exhibited modest growth inhibition with retention of viability that was associated with sustained induction of Cip1, extensive hypophosphorylation of retinoblastoma (Rb), and an accumulation of cells in G_1. In contrast, TPA induced death of MCF-7-PKC-α cells. MCF-7-PKC-α cells accumulated in G_2/M, transiently expressed only low levels of Cip1, and lacked a substantial degree of Rb hypophosphorylation. While eliciting only a modest cytostatic response in MCF-7 cells, bryostatin 1 exerted cytotoxic effects in MCF-7-PKC-α cells at low doses. This response was not seen at higher concentrations of this agent and high doses of bryostatin 1 inhibited MCF-7-PKC-α death induced by TPA. Preceding the onset of death and possibly involved in mediating this process, TPA-treated MCF-7-PKC-α cells expressed high levels of *gadd45* mRNA transcripts. Expression of *gadd45* was not induced by TPA in MCF-7 cells. Thus, associated with changes in PKC isoform expression was the conversion from a modest cytostatic effect observed in TPA-treated parental MCF-7 cells to death of MCF-7-PKC-α cells exposed to the phorbol ester.

Methods

Cell culture. MCF-7 cells were purchased from the American Type Culture Collection (Rockville, MD). MCF-7-PKC-α cells have been described elsewhere (16) and were generated by stably cotransfecting MCF-7 cells with PKC-α subcloned into the $pSV_2M(2)6$ vector (17) and a neomycin resistance plasmid. The stable transfectants were pooled and expanded as a heterogenous group. Cells stably transfected with the empty $pSV_2M(2)6$ vector were also generated (vector-transfected cells). Cells were grown in DME supplemented with 2 mM glutamine, 10 mM 4-[2-hydroxyethyl]-1-piperazinethanesulfonic acid, 10% fetal calf serum, 50 U/ml penicillin, and 50 μg/ml streptomycin. For cell growth experiments, 7.5×10^3 cells/ml were incubated in 24-well plates with replicates of 6 wells per treatment. Cell counts were done using a Coulter counter (Coulter Corp., Hialeah, FL). Bryostatin 1 was isolated from *Bugula neritina* as described (18).

Propidium iodide viability assay. Approximately 5×10^5 cells were resuspended in 1 ml of media. 20 μl of propidium iodide stock solution (500 μg/ml propidium iodide in 38 mM Na citrate solution) per milliliter of cell suspension was added to achieve a final propidium iodide concentration of 10 μg/ml. Samples were held at room temperature and analyzed immediately on a FACScan® flow cytometer (Becton Dickinson Immunocytometry Systems, Mountain View, CA). Statistical analysis was performed by simultaneously displaying on 2-parameter dot plots, red fluorescence versus forward scatter. Regions were assigned to the different populations displayed in the red fluorescence versus forward scatter histograms. The percentage of cells in each population was calculated using region statistics.

Microscopy. Cells maintained in culture were photographed at a magnification of 320 with a Nikon Diaphot inverted microscope. For structural analysis, cells were fixed for 30 min in 2.5% (vol/vol) glutaraldehyde and 0.1 M phosphate buffer (pH 7.4). After postfixation in 1% (wt/vol) osmium tetroxide, cells were dehydrated through a graded series of alcohol and propylene oxide and embedded in Epon. Thick sections were stained with Richardson's stain. Thin sections (< 90 nm) were stained with uranyl acetate and lead citrate and examined with a Jeol-1200 EX electron microscope.

DNA extraction and electrophoresis. Total cellular DNA was isolated as described previously, with minor revisions (19). Cells (1.5×10^7) were washed and resuspended in 0.5 ml of lysis buffer (50 mM Tris, 10 mM EDTA, 0.5% Triton X-100) with 5 mg/ml proteinase K and incubated at 37°C for 12 h. Lysates were then brought to a volume of 2.5 ml with lysis buffer and extracted twice with phenol-chloroform. DNA was then precipitated with 0.1 vol of 3 M sodium acetate and 3 vol of ethanol at −20°C for 12 h. DNA was resuspended in 10 mM Tris (pH 8.0) with 0.1 mM EDTA and digested with 0.2 mg of RNase A for 2 h at 37°C. Approximately 20 μg of each sample of total DNA was size fractionated on a 2% agarose gel, stained with ethidium bromide, and photographed by ultraviolet translumination to assess DNA fragmentation.

Cell cycle analysis. Cells were trypsinized, washed, resuspended in phosphate buffered saline, and fixed in 70% ethanol at 4°C for 30 min. Propidium iodide (50 μg/ml) in citrate buffer was added to the fixed cells and analysis was performed using a FACScan® flow cytometer. Analysis was done on 10^4 cells.

Northern blot analysis. Total RNA was extracted using TRIzol reagent (GIBCO BRL, Gaithersburg, MD) as per instructions of the manufacturer. Northern blot analysis was done as we have described previously (20). The p53 probe was purchased from the American Type Culture Collection. Other cDNA probes were kindly donated by Dr. Albert Fornace, Jr. (*gadd45*) and Dr. Steven Elledge (Cip1).

Western blot analysis. Hot Laemmli lysis buffer supplemented with 50 mM NaF was directly added to cells pelleted by centrifugation. The samples (10^5 cells/10 μl) were treated at 110°C for 5 min. Western blot analysis was performed as described previously (21) with 10^5 cells per lane. Antisera to p53 (Oncogene Science Inc., Manhasset, NY) and Rb (Santa Cruz Laboratories, Santa Cruz, CA) were used per instructions of their respective manufacturers. Enhanced chemiluminescence was used to detect the antigen–antibody complexes.

Southern blot analysis. DNA was extracted, exhaustively digested with BamHI, EcoR1, HindIII, and XbaI, subjected to agarose electrophoresis in a 0.6% gel, and transferred to filters. Random primer–labeled p53 was hybridized to the filters under standard conditions. Autoradiography was used to detect p53 digestion products.

Transient transfection analysis. This analysis was done as published elsewhere (21). Briefly, cells were plated 1 d before transfection. Calcium phosphate technique was used to transfect the cells with a reference β-galactosidase plasmid (3 μg), the chloramphenicol acetyl transferase (CAT) reporter construct (10 μg), and other appropriate cDNAs. The total DNA transfected was adjusted with carrier DNA to bring the final DNA content to 20 μg. After an overnight incubation, the cells were washed and placed in fresh media. Where indicated, phorbol esters were added after the cells were placed in fresh media. 40 h after transfection, extracts were prepared and β-galactosidase and CAT activities were determined (21). CAT values were normalized to β-galactosidase activity to control for variation in transfectional efficiency. Transfections were done in triplicate. The β-galactosidase plasmid was purchased from CLONTECH (Palo Alto, CA). The p53-responsive, PG-13-CAT reporter construct and its non–p53-responsive, mutated construct (MG-15-CAT) were generously donated by Dr. Bert Vogelstein. The p53 promoter-CAT reporter construct (p0.5 CAT) and wild-type and mutant p53 expression constructs have been described previously (22).

Nuclear run-on analysis. Nuclei (250 μg) extracted by standard techniques and 250 μCi [α-^{32}P]UTP were used for run-on transcription assays. Using previously published techniques (23), equal concentrations of ^{32}P-labeled RNA were hybridized to Hybond-N filters on which the appropriate cDNA fragments (2 μg/slot) had been hybridized. Hybridization of nascent RNA was normalized to the genomic signal. Quantitation of the signal was performed using a PhosphorImager (Molecular Dynamics, Inc., Sunnyvale, CA) with Image Quant™ software. Transforming growth factor-β cDNA obtained from the American Type Culture Collection was used as an internal control since its expression was not altered in MCF-7-PKC-α cells nor in MCF-7 cells by TPA treatment (data not shown).

Results

MCF-7-PKC-α cells undergo death in response to TPA. In the absence of TPA, MCF-7-PKC-α cells proliferated at a higher rate than did vector-transfected or MCF-7 cells (MCF-7,

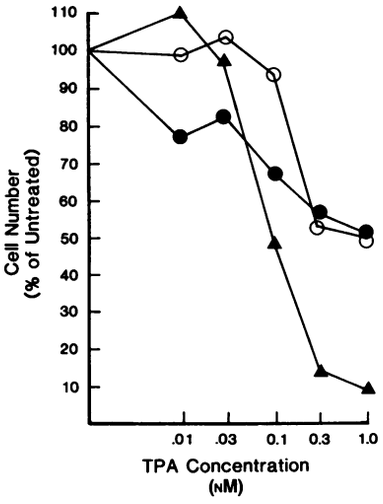

Figure 1. Effects of TPA on growth of MCF-7 and MCF-7-PKC-α cells. MCF-7 (●), vector-transfected (○), and MCF-7-PKC-α (▲) cells were plated at 7.5×10^3/ml in 24-well plates and treated with varying TPA concentrations. Cell counts were done 5 d later. Cell numbers are expressed as a percentage relative to their non-TPA-treated stable cells with 100% equal to the cell number in vehicle-treated groups. Each point presents six replicates within a single experiment. Similar results were obtained in another study.

64,200; vector-transfected, 67,920; and MCF-7-PKC-α, 379,250 cells after 5 d in non-TPA-containing media). In response to phorbol ester treatment, growth of MCF-7 and vector-transfected cells was modestly decreased (Fig. 1). While proliferation of MCF-7-PKC-α cells was inhibited to a greater degree than in parental and vector-transfected MCF-7 cells, the sensitivity of parental/vector-transfected MCF-7 and MCF-7-PKC-α cells to phorbol ester-induced growth inhibition was similar.

To examine whether differences in the rate of cell death were responsible for the enhancement in TPA-induced growth inhibition of MCF-7-PKC-α cells, the viability status of phorbol ester-treated cells was examined. Due to extensive clumping of nonadherent, TPA-treated MCF-7-PKC-α cells, it was difficult to quantitate cellular viability using trypan blue exclusion. Viability of cells was examined by FACS® analysis using propidium iodide exclusion as a measure of cellular integrity (24). Flow cytometric analysis provided a better dispersion of cells and allowed a more precise means to quantitate viability. Viable cells exclude propidium iodide and display an appropriate degree of forward scatter for an intact cell (see R2 gate in Fig. 2). Other populations of cells display either an intense increase in propidium iodide uptake with large variations in forward scatter (see R1 gate in Fig. 2) or a moderate increase in propidium iodide uptake with varying decreases in forward scatter (see R3 gate in Fig. 2). The increase in propidium iodide uptake of cells gating into the R1 and R3 regions is consistent with loss of membrane integrity while the reduced forward scatter suggests either cellular condensation or fragmentation. Microscopic analysis of cells sorted from these regions demonstrated that intact, normal appearing cells were contained in the R2 region while debris with stripped nuclei and significantly condensed cells were found in the R1 and R3 regions, respectively (data not shown).

In untreated MCF-7 and MCF-7-PKC-α cells, the vast majority of cells excluded propidium iodide and displayed a degree of forward light scatter indicative of an intact cell (see R2 region in Fig. 2, *A* and *C*). After a 72-h exposure to 10 nM TPA, the majority of parental MCF-7 cells excluded propidium iodide and displayed approximately the same size characteristics as did untreated cells (Fig. 2*B*). The proportion of events gated into the R1 and R3 regions in TPA-treated parental MCF-7 cells was not significantly increased. In contrast, TPA-treated MCF-7-PKC-α cells displayed a significant reduction in viable, propidium iodide-excluding cells gating into the R2 region. A significant proportion of MCF-7-PKC-α cells exposed to TPA developed either an intense increase in propidium iodide uptake (R1 region) or a moderate increase in propidium iodide uptake with a reduction in forward scatter (R3 region). Qualitatively similar decreases in membrane integrity and loss of viability were observed in TPA-treated MCF-7-PKC-α cells using trypan blue exclusion (data not shown). A significant decrease in viability of MCF-7-PKC-α cells exposed to 10 nM TPA, as defined by a loss of propidium iodide-excluding cells gated to the R1 region, was observed after a 12-h exposure to 10 nM TPA and was maximal after a 24-48-h exposure to this agent (Fig. 3*A*). In contrast, only minimal decreases in viability of parental or vector-transfected cells were seen after TPA treatment. After a 48-h exposure, MCF-7-PKC-α cell death was maximal at a TPA concentration of 10 nM (Fig. 3*B*). Thus, increases in cell death were responsible for the more profound growth inhibition observed in TPA-treated MCF-7-PKC-α cells.

Bryostatin 1 displays concentration-dependent, biphasic effects on growth of MCF-7-PKC-α cells. Bryostatin 1, a macrocyclic lactone, has completed phase I trials and is currently undergoing clinical evaluation as an antineoplastic agent in phase II studies (25, 26). While bryostatin 1 is believed to exert its effects by activating the PKC pathway, it can either mimic or antagonize the effects of phorbol esters in a cell-specific fashion (27). In certain cell types, effects exerted by bryostatin 1 at low doses dissipate as the concentration is increased (28-32). The dose- and cell type-specific responses of bryostatin 1 are thought to be due to preferential up- or downregulation of specific isoforms involved in mediating the effects of TPA and bryostatin 1 (28-33).

While eliciting only minimal growth inhibition in parental MCF-7 cells that waned at higher concentrations (Fig. 4 *A*), bryostatin 1 displayed significant, concentration-dependent antiproliferative effects in MCF-7-PKC-α cells (Fig. 4 *B*). The maximal degree of MCF-7-PKC-α growth inhibition induced by TPA was reached at a concentration of 1 nM and remained constant with exposures of 1,000 nM (Fig. 4 *B*). In contrast, the growth inhibitory effects of bryostatin 1 significantly waned at concentrations $\geq$100 nM. To examine whether growth inhibition of MCF-7 and MCF-7-PKC-α cells induced by bryostatin 1 was due to a cytostatic or cytotoxic mechanism, cellular viability was examined (Fig. 4, *C* and *D*). MCF-7 cells retained viability upon exposure to 10 nM TPA or bryostatin 1, a concentration that maximally inhibited growth of these cells (Fig. 4 *C*). In contrast, MCF-7-PKC-α cells displayed a temporally dependent reduction in viability when exposed to either 10 nM TPA or bryostatin 1 (Fig. 4 *D*). As with TPA, MCF-7 and MCF-7-PKC-α cells responded to low doses of bryostatin 1 in qualitatively dissimilar fashions exhibiting cytostatic and cytotoxic responses, respectively.

The ability of high bryostatin 1 concentrations to interfere with TPA-induced death of MCF-7-PKC-α cells was examined. TPA significantly inhibited growth and reduced the viability of MCF-7-PKC-α cells (Fig. 5, *A* and *B*, respectively). Incubation with 1,000 nM bryostatin 1 inhibited growth of MCF-7-PKC-α cells but not to the extent seen with TPA treatment (Fig. 5

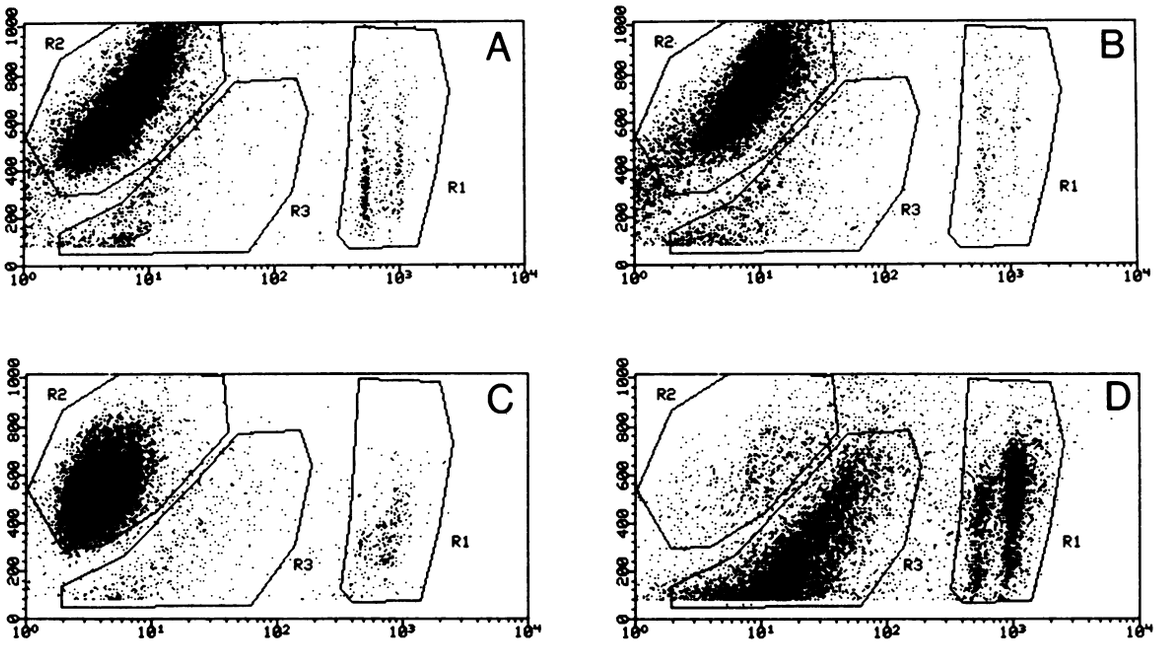

Figure 2. TPA treatment induces death of MCF-7-PKC-α cells. MCF-7 (*A* and *B*) and MCF-7-PKC-α cells (*C* and *D*) were treated with vehicle (*A* and *C*) or 10 nM TPA (*B* and *D*) for 72 h. Cells were harvested and exposed to propidium iodide. Forward light scatter (see ordinate) and propidium iodide uptake (see abscissa) were measured. Cells were gated into separate areas representing: R1, high propidium iodide uptake with variable forward scatter; R2, low propidium iodide uptake and appropriate forward scatter for intact cells; and R3, reduced forward scatter consistent with debris and/or enhanced propidium iodide uptake. This experiment was repeated with similar results. Vector-transfected cells gave identical results to MCF-7 cells.

A). Unlike the extensive cell death that occurred after exposure to 10 nM bryostatin 1, viability of MCF-7-PKC-α cells treated with 1,000 nM bryostatin 1 was essentially unaffected and comparable to that of vehicle-treated cells (Fig. 5 *B*). In cells coincubated with these agents, high concentrations of bryostatin 1 exerted dominant effects over TPA and blocked death induced by the phorbol ester. Growth and viability of cells coincubated with these agents was identical to that seen in MCF-7-PKC-α cells treated only with 1,000 nM bryostatin 1 (Fig. 5, *A* and *B*). Thus, high concentrations of bryostatin 1 were able to interfere with the signal transduction pathway used by TPA to induce MCF-7-PKC-α cell death.

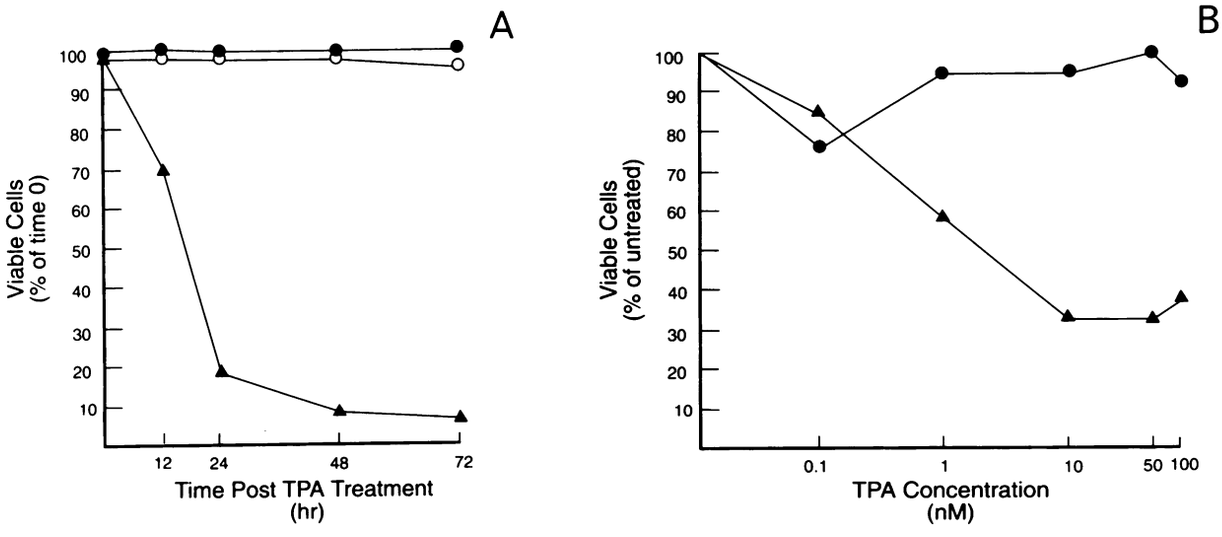

Figure 3. Time- and concentration-dependent death of TPA-treated MCF-7 cells. MCF-7 (●), vector-transfected (○), and MCF-7-PKC-α (▲) cells were treated with 10 nM TPA for varying times (*A*) or varying TPA concentrations for 24 h (*B*). Cellular viability was measured using the propidium iodide exclusion assay with viable cells defined as those gating into the R2 region that exclude propidium iodide and display the appropriate degree of forward scatter for an intact cell. Viable cell number is expressed on the ordinate with 100% equaling the percentage of non–TPA-treated cells gating to the R2 region. These experiments were repeated with similar results.

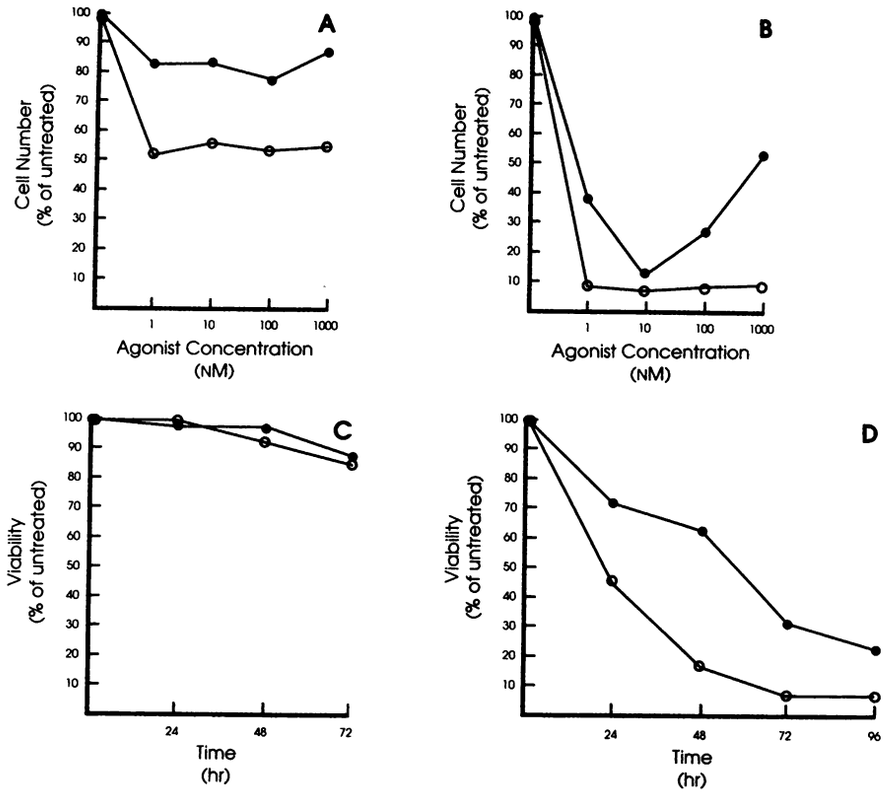

Figure 4. Effects of bryostatin 1 on MCF-7 and MCF-7-PKC-α cell growth and viability. MCF-7 (*A*) and MCF-7-PKC-α (*B*) cells were exposed to varying concentrations of TPA (○) or bryostatin 1 (●) (see abscissa) and cell counts were done 5 d after treatment. MCF-7 (*C*) and MCF-7-PKC-α (*D*) cells were treated with 10 nM TPA (○) or bryostatin 1 (●) for varying times (see abscissa) and cell viability was measured. Viability is expressed as a percentage of total cell number with 100% equaling the viability of untreated cells. Replicates of six and three were obtained for each point representing cell counts and viability determinations, respectively. Similar results were obtained in other experiments. Vector-transfected cells gave similar results to those obtained with parental MCF-7 cells.

Morphologic changes associated with TPA-induced death of MCF-7-PKC-α cells occur in the absence of DNA degradation into oligonucleosomal units. MCF-7 cells grew adherent to the plastic surface and exhibited an epithelioid appearance (Fig. 6 *A*). TPA treatment caused the cell to flatten (Fig. 6 *B*) with retention of the normal cellular architecture. MCF-7-PKC-α cells proliferated in suspension devoid of an epithelioid morphology (Fig. 6 *C*). Exposure of MCF-7-PKC-α cells to TPA

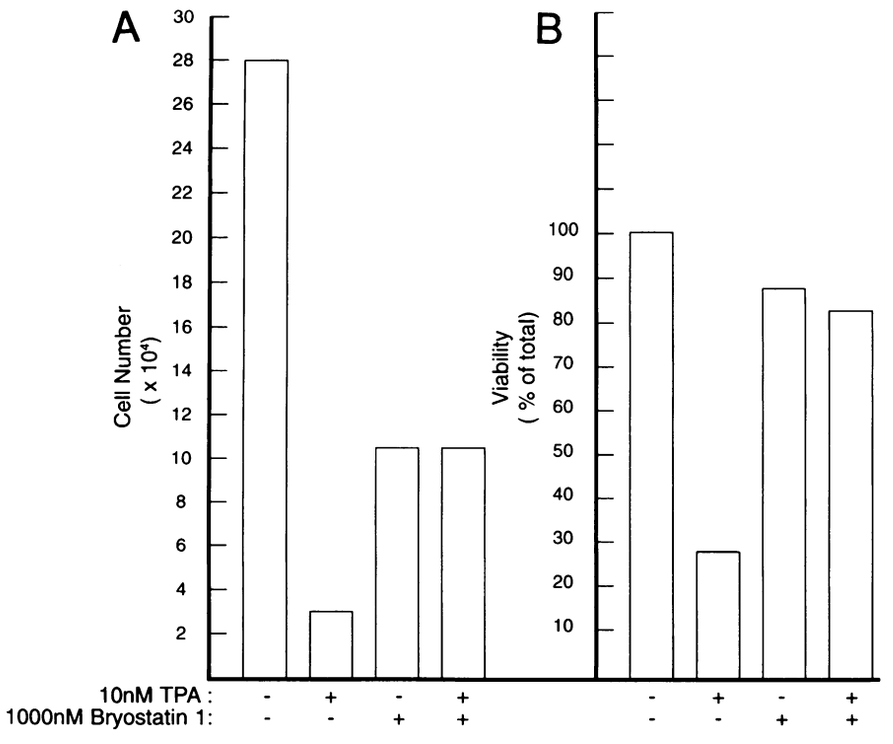

Figure 5. High concentrations of bryostatin 1 inhibit TPA-induced death of MCF-7-PKC-α cells. MCF-7-PKC-α cells were exposed for 5 d to vehicle, 10 nM TPA, 1,000 nM bryostatin 1, or both agents (see below the figure). In cells treated with both agents, bryostatin 1 was added 6 h before TPA. Cell counts (*A*) and viability determinations (*B*) were done. Replicates of six and three were obtained for each point representing cell counts and viability determinations, respectively. Similar results were obtained in separate experiments.

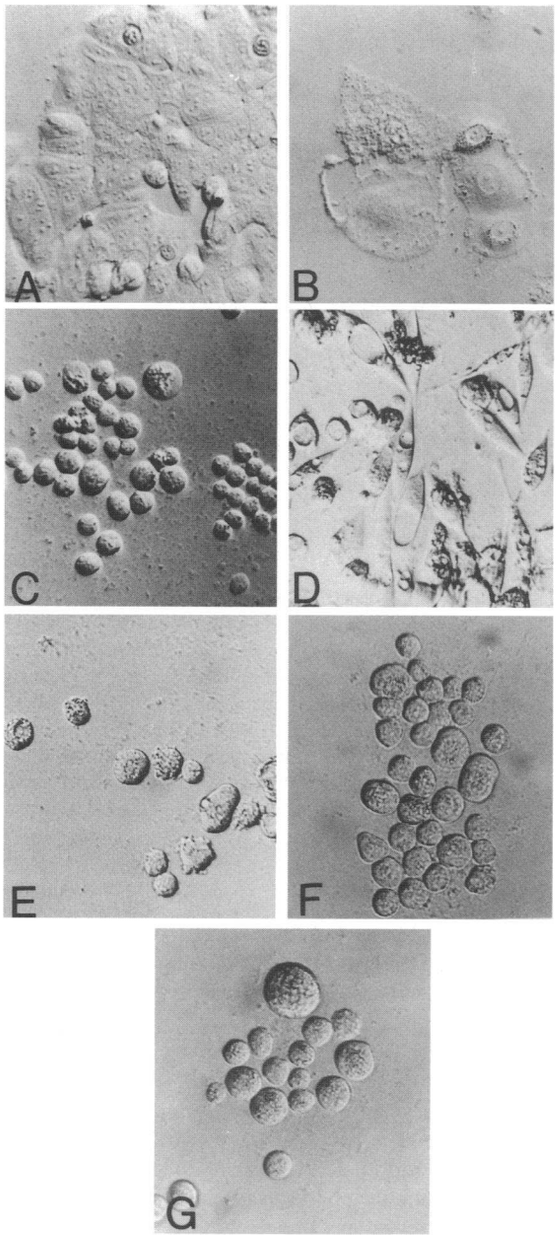

Figure 6. TPA- and bryostatin 1–induced morphologic changes in MCF-7-PKC-α cells. Inverted microscopy was done on vehicle-treated MCF-7 (*A*) and MCF-7-PKC-α (*C*). MCF-7 and MCF-7-PKC-α cells treated with 100 nM TPA for 72 h are shown in *B* and *D*, respectively. Microscopic analysis was also performed on MCF-7-PKC-α cells treated for 72 h with 10 nM bryostatin 1 (*E*) and 1,000 nM bryostatin 1 in the absence (*F*) or presence (*G*) of 10 nM TPA. When coincubated with TPA, bryostatin 1 was added 6 h before the phorbol ester. Similar observations were made in other experiments. Vector transfected MCF-7 cells behaved in an identical fashion to MCF-7 cells in response to TPA.

was associated with extensive clumping (data not shown) and vacuolization (Fig. 6 *D*). A minority of TPA-treated MCF-7-PKC-α cells adhered tightly to the plastic surface, displayed prominent vacuolization, and assumed a fibroblast-like appearance (Fig. 6 *D*). Exposure to 10 nM bryostatin 1 induced only rare fibroblast-like adherent cells and a much lesser degree of vacuole formation (Fig. 6 *E*). Small evaginations from the plasma membrane were seen in cells treated with 10 nM bryostatin 1 (Fig. 6 *E*). MCF-7-PKC-α cells treated with 1,000 nM bryostatin 1 in the absence (Fig. 6 *F*) or presence (Fig. 6 *G*) of 10 nM TPA closely resembled untreated MCF-7-PKC-α cells. In addition, the plasma membrane evaginations seen in cells treated with doses of bryostatin 1 inducing death (10 nM) were not evident in cells treated with high concentrations of this agent. Thus, high doses of bryostatin 1 failed to elicit the same effects seen with lower concentrations of this agent and exerted dominant effects over TPA-induced morphologic changes in MCF-7-PKC-α cells.

Using Richardson's stain, sectioned MCF-7 (Fig. 7 *A*) and MCF-7-PKC-α (Fig. 7 *B*) cells were examined. TPA treatment of MCF-7-PKC-α cells was associated with nuclear and cellular condensation and cell blebbing (Fig. 7 *B*). Similar changes were not seen in TPA-treated MCF-7 cells (Fig. 7 *A*). Thus, in contrast to MCF-7 cells, MCF-7-PKC-α cells displayed certain signs indicative of apoptosis (e.g., cellular/nuclear condensation plasma membrane and blebbing) in response to TPA. Electron microscopy indicated that the extensive vacuolization of TPA-treated MCF-7-PKC-α cells was due to lysosomal swelling (Fig. 7 *C*). The role, if any, of the lysosomal enlargement in TPA-induced apoptosis of MCF-7-PKC-α cells is uncertain. Although the development of translucent cytoplasmic vacuoles has been described in apoptosis, lysosomal swelling to the degree observed in TPA-treated MCF-7-PKC-α cells is not usually considered as a morphologic feature of apoptosis (34). Treatment with 10 nM bryostatin 1 which produced a similar degree of MCF-7-PKC-α death as did 10 nM TPA (Fig. 4 *D*) was associated with a much lesser degree of lysosomal swelling (Fig. 6 *E*). As assessed by staining sectioned cells with Richardson's stain, low-dose bryostatin 1 treatment produced the same cell blebbing (possibly corresponding to the plasma membrane evaginations seen with inverted microscopy) and cellular/nuclear condensation (data not shown). The lysosomal swelling seen in TPA-treated MCF-7-PKC-α cells could be a unique morphologic feature associated with the death of these cells. Alternatively, this event could be due to the differences in PKC isoform expression between MCF-7-PKC-α and MCF-7 cells and their effect on the lysosomal response to TPA-induced activation. However, the ability of 10 nM TPA and bryostatin 1 to elicit different degrees of lysosomal swelling in MCF-7-PKC-α cells and yet to stimulate a similar extent of cell death suggests that the pronounced swelling was due to a primary alteration in the lysosomal response to TPA rather than being associated with the death process.

Given the association of DNA fragmentation into oligonucleosomal units with apoptosis, this parameter was examined in MCF-7-PKC-α cells (Fig. 8). Despite the morphologic evidence suggestive of apoptosis in TPA-treated MCF-7-PKC-α cells, degradation of DNA into oligonucleosomal units was not detected after phorbol ester treatment of these cells. Certain cells undergoing apoptosis have been reported to exhibit DNA degradation yielding high molecular weight fragments in the absence of further degradation to form oligonucleosomal units (35). Thus our inability to detect DNA degradation into oligonucleosomal units does not necessarily imply the absence of DNA fragmentation in TPA-treated MCF-7-PKC-α cells.

TPA induces dissimilar cell cycle alterations in MCF-7 and MCF-7-PKC-α cells. A time-dependent accumulation of MCF-7 cells in G_1 was observed with TPA treatment (Fig. 9 *A*). In contrast, TPA treatment elicited a prominent accumulation of

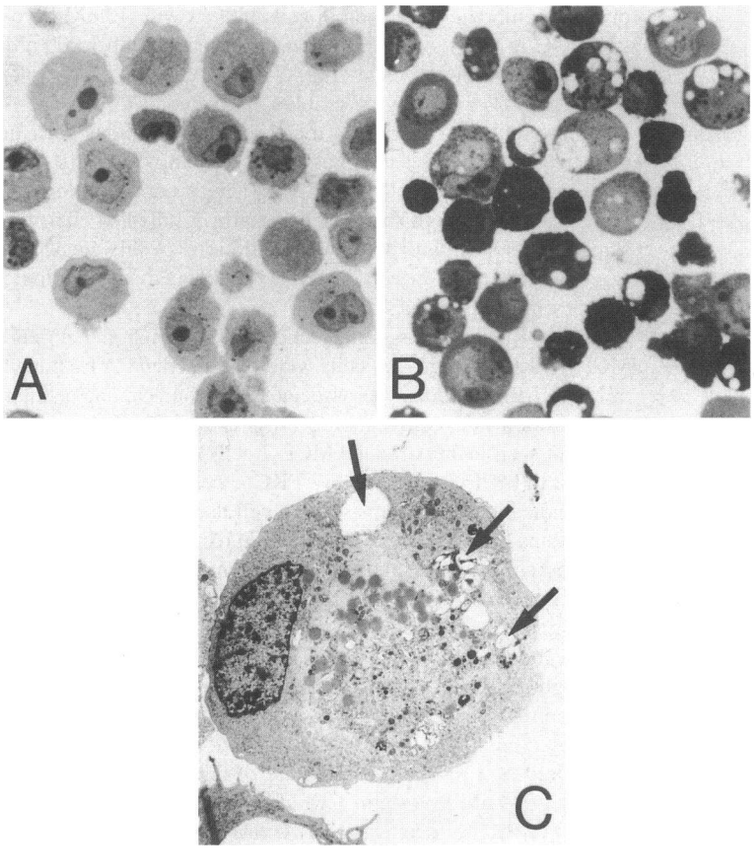

Figure 7. TPA-treated MCF-7-PKC-α cells display cellular condensation and prominent vacuole formation. MCF-7 (*A*) and MCF-7-PKC-α (*B*) cells were treated with 10 nM TPA for 72 h. Staining of sectioned cells was done with Richardson's stain. In *C*, electron microscopy was done on MCF-7-PKC-α cells treated with 10 nM TPA for 72 h. The arrows in *C* indicate the swollen lysosomes. Similar results were obtained in separate experiments. Vector-transfected cells responded to TPA treatment in a similar manner as did MCF-7 cells.

MCF-7-PKC-α cells in G_2/M (Fig. 9 *B*). Thus, the dissimilar response of MCF-7 and MCF-7-PKC-α cells to TPA suggested that differences exist in the factors mediating phorbol ester–induced modulation of cell cycle check points.

MCF-7-PKC-α cells lack p53. Given the prominent role of p53 in controlling cell cycle progression from G_1 to S phase and its ability to stimulate cell death (36–38), the status of this protein in MCF-7 and MCF-7-PKC-α cells was assessed. Using Northern blot analysis, p53 mRNA transcripts were readily detected in vector-transfected and MCF-7 cells (Fig. 10). However, levels of p53 mRNA transcripts were negligible in MCF-7-PKC-α cells (Fig. 10 *A*). Using Western blot analysis, a concomitant reduction in the content of p53 protein was observed in MCF-7-PKC-α cells relative to those levels found in MCF-7 and vector-transfected cells (Fig. 10 *B*). To examine whether a gross p53 gene rearrangement occurred in MCF-7-PKC-α cells that could explain its loss of expression, Southern blot analysis was performed. The use of multiple restriction enzymes that cut within the p53 locus (BamHI, EcoRI, HindIII, and XbaI) failed to reveal any gross rearrangement of the p53 gene (data not shown). To directly assess the transcriptional status of factors controlling expression of p53, transient transfection assays were performed using a p53 promoter–reporter CAT construct (p0.5 CAT). The p53 promoter region subcloned into the reporter construct includes nucleotides −320 to +210 relative to the transcriptional start site and has been shown to be activated by p53 (22). After normalization to β-galactosidase activity to control for differences in transfectional efficiency, a significant basal induction of CAT expression controlled by the p53 promoter was evident in MCF-7 cells (Fig. 11 *A*). In MCF-7-PKC-α cells, basal levels of p0.5 CAT activity were negligible (Fig. 11 *A*). Transient overexpression of p53 in MCF-7 cells further enhanced activity of p0.5 CAT while expression of an inactive p53 mutant did not significantly stimulate p0.5 CAT activity. In MCF-7-PKC-α cells, expression of p53 stimulated p0.5 CAT activity to a lower absolute level than in MCF-7 cells but to a similar degree relative to the fold increase over basal (three- and sixfold over basal in MCF-7 and MCF-7-PKC-α cells, respectively). Stimulation of p0.5

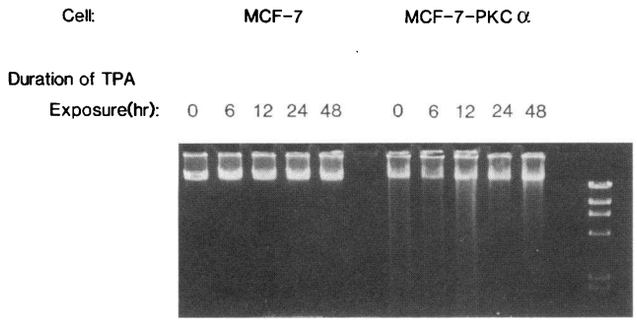

Figure 8. TPA-treated MCF-7-PKC-α cells undergo death without forming an oligonucleosomal DNA ladder. MCF-7 and MCF-7-PKC-α cells were treated for varying times with 100 nM TPA (see above the gel). DNA was extracted and subjected to agarose electrophoresis. The migration of molecular weight indicators is shown on the far right. This experiment was repeated on several occasions with similar results. Vector-transfected cells responded to TPA treatment in a similar manner as did MCF-7 cells.

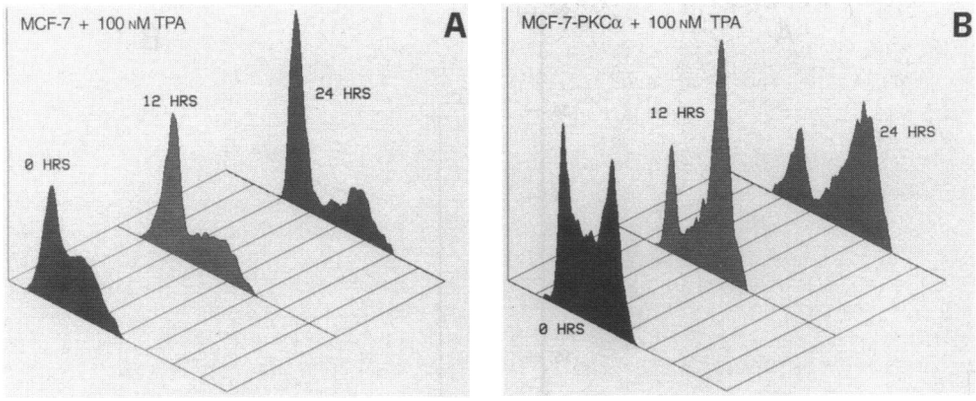

Figure 9. Cell cycle differences in TPA-treated MCF-7 and MCF-7-PKC-α cells. MCF-7 (*A*) and MCF-7-PKC-α (*B*) cells were treated with 100 nM TPA for varying periods of time indicated above the histograms, and cell cycle distribution was analyzed by propidium iodide staining. These results were obtained in other experiments. Vector-transfected cells gave results identical to those obtained with MCF-7 cells.

CAT activity by p53 expression in MCF-7-PKC-α cells was specific since cotransfection with the inactive p53 mutant failed to enhance this activity. Thus, the marked reduction in p53 mRNA transcripts contained in MCF-7-PKC-α cells could, in part, be explained by a reduction in the transcription of this gene as indicated by the decreased p53–promoter CAT reporter activity in these cells.

Functional p53 activity was assessed using the PG-13-CAT construct that contains multiple copies of the consensus p53 response element. In MCF-7 cells transiently transfected with the PG-13-CAT construct, significant activation of the reporter was evident (Fig. 11 *B*). MCF-7 cells transfected with the mutant, non–p53-responsive construct (MG-15-CAT) displayed negligible levels of CAT activity. In MCF-7-PKC-α cells, similar low levels of CAT activity were expressed from either PG-13-CAT or MG-15-CAT. Thus, MCF-7-PKC-α cells displayed a large reduction in functional p53-directed transcriptional activity.

Phorbol esters induce Cip1 expression in MCF-7 cells while gadd45 is strongly induced in MCF-7-PKC-α cells. Given the ability of Cip1/WAF1/p21 to arrest cells in G_0/G_1 (39, 40) and the association of Cip1 and *gadd45* expression with cell death (41–45), we examined their expression in TPA-treated MCF-7 and MCF-7-PKC-α cells (Fig. 12). TPA-treated MCF-7 cells displayed a significant induction of Cip1 that temporally coincided with growth arrest and accumulation of cells in G_1 (Fig. 12 *A*). A modest induction of Cip1 was detected in TPA-treated MCF-7-PKC-α cells. However, TPA failed to stimulate a sustained expression of Cip1 in MCF-7-PKC-α cells. In contrast, TPA treatment of MCF-7-PKC-α cells markedly stimulated expression of *gadd45* (Fig. 12 *A*). Only a modest TPA-induced increase in *gadd45* was detected in MCF-7 cells. The increase in *gadd45* in MCF-7-PKC-α cells (2–4 h) temporally preceded the onset of decreases in viability occurring at 12 h (Fig. 3 *A*). Using nuclear run-on analysis, basal transcriptional activity of *gadd45* was shown to be significantly increased (≈ 8.8-fold) in MCF-7-PKC-α cells relative to MCF-7 cells (Fig. 12 *B*). While *gadd45* transcription was not stimulated by TPA in MCF-7 cells, a 2.6-fold increase in transcription of this gene was observed in MCF-7-PKC-α cells within a 30-min exposure to TPA (Fig. 12 *B*). Transcription of *gadd45* in MCF-7-PKC-α cells remained elevated above the basal levels even 12 h after exposure to TPA. The inability of TPA to induce *gadd45* expression in MCF-7-PKC-α cells pretreated with cycloheximide demonstrated that induction of this gene required ongoing protein synthesis (Fig. 12 *C*).

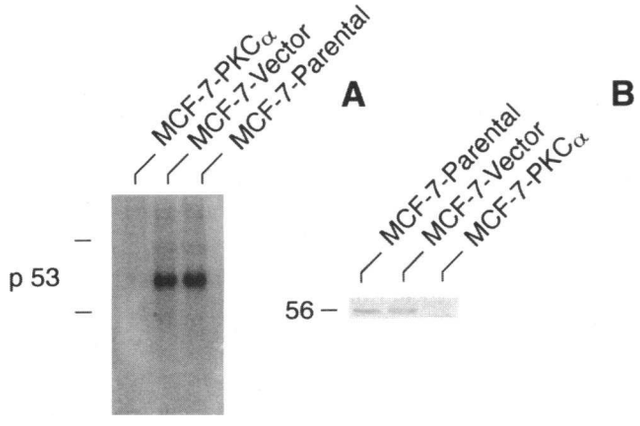

Figure 10. MCF-7-PKC-α cells exhibit decreases in p53 content. Northern (*A*) and Western (*B*) blot analysis were done on MCF-7-PKC-α, MCF-7 vector-transfected, and MCF-7 cells. The derivation of the samples is indicated above the autoradiograms. Each experiment was repeated with similar results.

TPA-induced expression of Cip1 in MCF-7 cells was not associated with an increase in p53-dependent transcriptional activity. Expression of Cip1 and *gadd45* can be mediated by a p53-dependent pathway (39–41, 46, 47). To examine whether TPA used a p53-dependent mechanism to induce expression of these genes, the content of p53 and functional status of this pathway were analyzed in TPA-treated cells. TPA treatment of MCF-7 cells elicited a temporally dependent reduction in p53 mRNA transcripts (Fig. 13 *A*). In MCF-7-PKC-α cells, p53 mRNA transcripts were not detected in the basal state nor were they induced upon TPA treatment. To assess the functional consequences of the TPA-induced reduction in p53 mRNA transcripts in MCF-7 cells, expression of the p53-responsive PG-13-CAT construct was examined after TPA treatment (Fig. 13, *B* and *C*). Treatment of MCF-7 cells with 10 or 100 nM TPA reduced the activity of the p53-responsive, PG-13-CAT construct (Fig. 13 *C*). Given the possibility that TPA may acutely activate and then later repress p53-dependent transcriptional activity, the effects of varying the duration of TPA exposure to MCF-7 cells transiently transfected with the PG-13 reporter were examined. Whether added for the entire period (48 h) or only the final 24 h, TPA did not activate the PG-13 reporter construct and, in fact, possessed significant inhibitory properties (Fig. 13 *C*). Under these treatment conditions, TPA did not

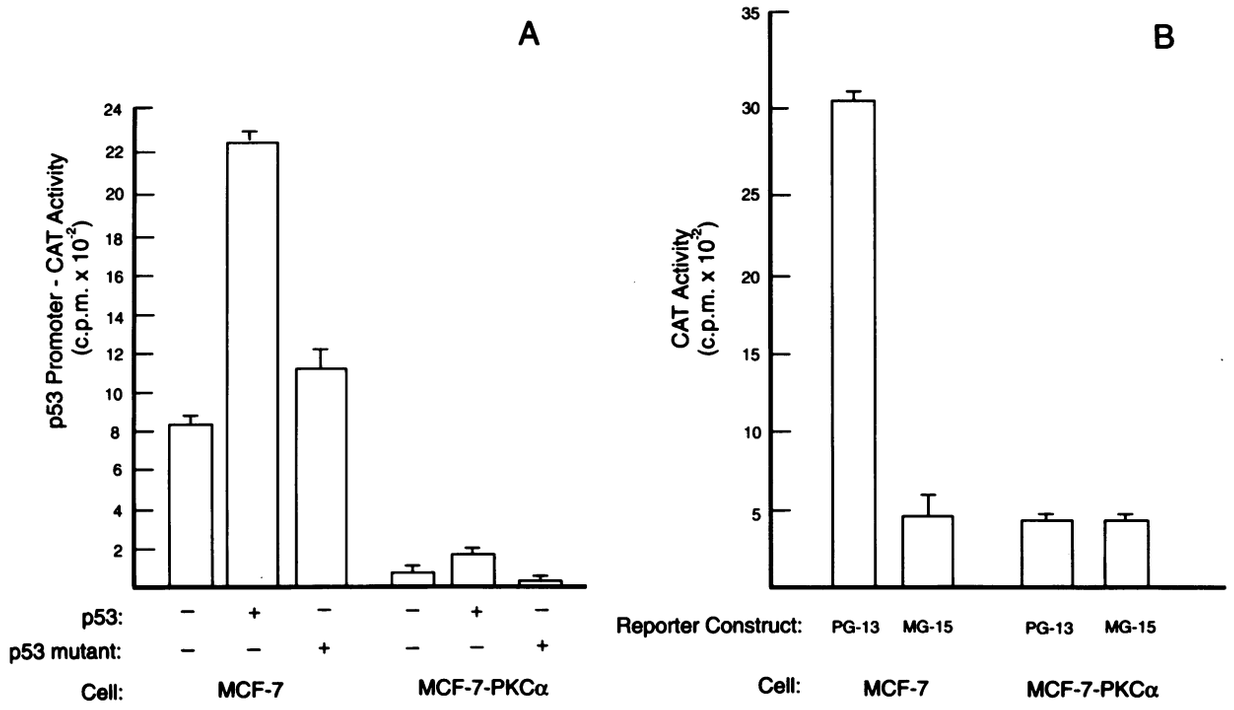

Figure 11. MCF-7-PKC-α cells display reductions in p53 functional activity. In *A*, MCF-7 and MCF-7-PKC-α cells (see below the figure) were transiently cotransfected with p.05 CAT reporter and β-galactosidase reference plasmid in the absence or presence of p53 wild-type or mutant expression vectors (see below figure). CAT activity was normalized to β-galactosidase levels and is shown on the ordinate. In *B*, MCF-7 and MCF-7-PKC-α cells (see below the figure) were transiently cotransfected with the p53-responsive PG-13-CAT or a mutated, non-p53-responsive MG-15-CAT reporter and a β-galactosidase plasmid. CAT results were normalized to β-galactosidase activity. These experiments were repeated with similar findings. Vector-transfected cells gave similar results to those obtained with MCF-7 cells.

stimulate activation of the PG-13-CAT reporter construct. Thus, despite the significant Cip1 induction in TPA-treated MCF-7 cells, p53-dependent transcriptional activity diminished after exposure to the phorbol ester.

Rb hypophosphorylation in TPA-treated MCF-7 and MCF-7-PKC-α cells. Cip1 inhibition of the cyclin-dependent kinase activities leading to a reduced level of Rb phosphorylation is involved in mediating growth arrest at the G_1-S boundary (48). To examine whether differences in Rb phosphorylation could explain the altered cell cycle progression in TPA-treated MCF-7-PKC-α cells, Western blot analysis was done to determine the phosphorylation status of this protein (Fig. 14). Nearly complete hypophosphorylation of Rb was induced by TPA treatment in MCF-7 cells. In contrast, TPA treatment of MCF-7-PKC-α cells produced only a partial degree of Rb hypophosphorylation. Thus, extensive hypophosphorylation of Rb in TPA-treated MCF-7 cells was associated with sustained, high levels of Cip1 expression. In addition, the increase in Cip1 expression preceded the onset of Rb hypophosphorylation in MCF-7 cells. The transient expression of Cip1 in TPA-treated MCF-7-PKC-α cells at only 4 and 8 h after TPA exposure was associated with a much reduced degree of Rb hypophosphorylation relative to that seen in parental MCF-7 cells. It is unclear as to whether the lesser degree of induction or the transient nature of Cip1 expression was responsible for the lesser degree of Rb hypophosphorylation in TPA-treated MCF-7-PKC-α cells.

Discussion

In MCF-7 cells, phorbol esters and, to a lesser degree, bryostatin 1 elicit a modest degree of growth inhibition associated with retention of viability. However, overexpression of PKC-α in MCF-7 breast cancer cells, either directly or indirectly due to other phenotypic alterations occurring in these cells, lead to cell death in response to phorbol esters and low doses of bryostatin 1 rather than the cytostatic effect elicited in the parental MCF-7 cell. It remains unresolved as to whether overexpression of PKC-α or the concurrent alterations in the endogenous expression of other PKC isoforms are responsible for initiating the death signal. Although generated by overexpression of PKC-α, MCF-7-PKC-α cells display increases in the β and θ isoforms, moderate decreases in PKC-δ and -ι, and a total abolition of PKC-η expression (reference 16 and manuscript in preparation). Thus, with these concomitant alterations in other PKCs, it is difficult from the current data to ascribe a direct role for α or another specific isoform in stimulating death. Lastly, it remains to be determined whether the mechanisms responsible for the dissimilar response of TPA-treated MCF-7-PKC-α cells reside solely within the PKC pathway or are due to alterations in signaling pathways distal to and stimulated by PKC activation that regulate induction of death. Nonetheless, these data suggest that alterations in PKC isoform expression can influence the molecular switch controlling the decision of a breast cancer cell to undergo death or differentiation in response to activation of this pathway.

The ability of bryostatin 1 to exert effects at low doses that wane or disappear at higher doses has been amply documented in various cell types (27–32). In addition, the capacity for high doses of bryostatin 1 to antagonize the cellular effects of TPA has been described previously (27–29, 32, 33). Thus, similar concentration-dependent responses and dominant effects over

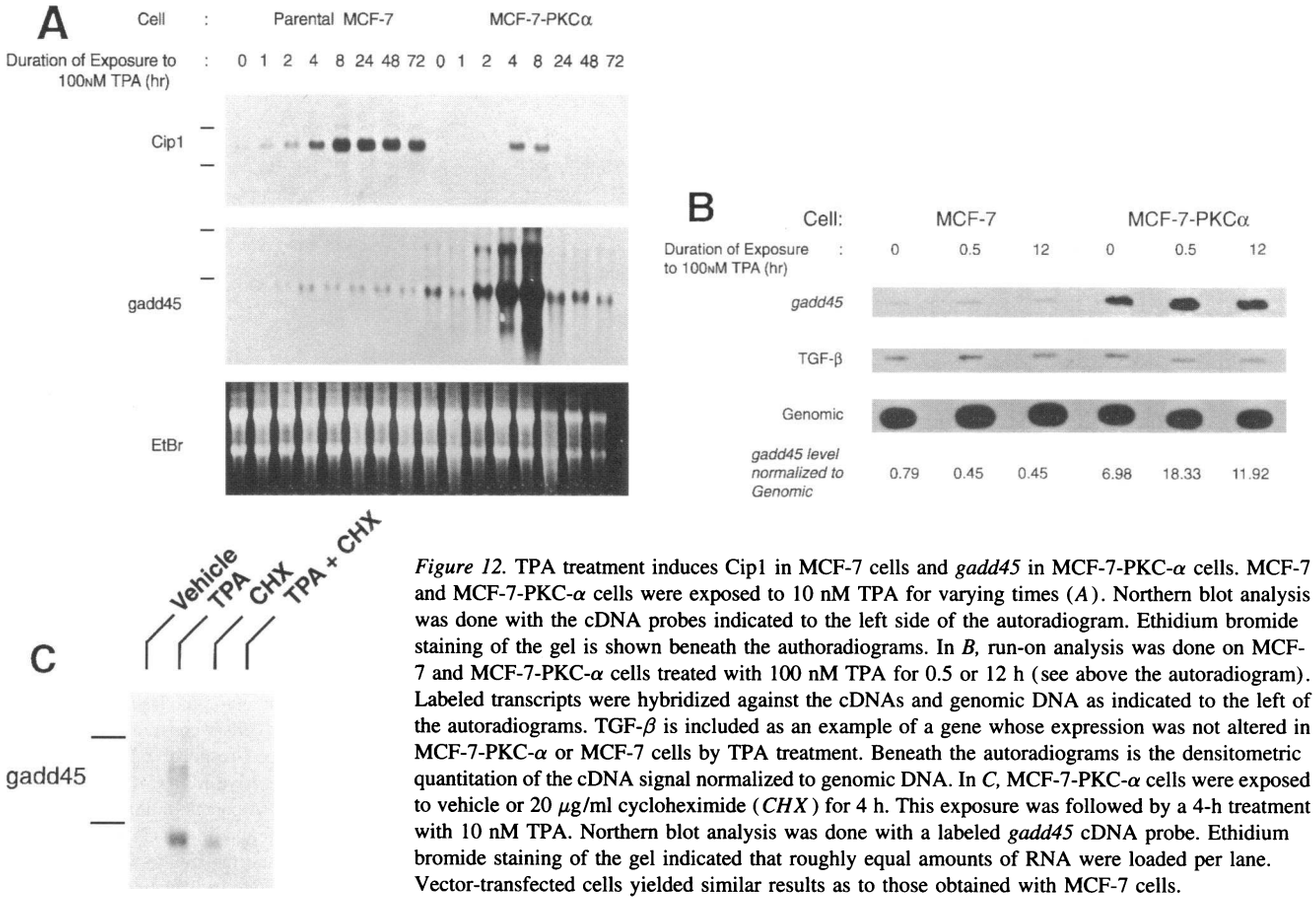

Figure 12. TPA treatment induces Cip1 in MCF-7 cells and *gadd45* in MCF-7-PKC-α cells. MCF-7 and MCF-7-PKC-α cells were exposed to 10 nM TPA for varying times (*A*). Northern blot analysis was done with the cDNA probes indicated to the left side of the autoradiogram. Ethidium bromide staining of the gel is shown beneath the authoradiograms. In *B*, run-on analysis was done on MCF-7 and MCF-7-PKC-α cells treated with 100 nM TPA for 0.5 or 12 h (see above the autoradiogram). Labeled transcripts were hybridized against the cDNAs and genomic DNA as indicated to the left of the autoradiograms. TGF-β is included as an example of a gene whose expression was not altered in MCF-7-PKC-α or MCF-7 cells by TPA treatment. Beneath the autoradiograms is the densitometric quantitation of the cDNA signal normalized to genomic DNA. In *C*, MCF-7-PKC-α cells were exposed to vehicle or 20 μg/ml cycloheximide (*CHX*) for 4 h. This exposure was followed by a 4-h treatment with 10 nM TPA. Northern blot analysis was done with a labeled *gadd45* cDNA probe. Ethidium bromide staining of the gel indicated that roughly equal amounts of RNA were loaded per lane. Vector-transfected cells yielded similar results as to those obtained with MCF-7 cells.

TPA to those elicited by bryostatin 1 in MCF-7-PKC-α cells have been reported in other cell types. The molecular mechanisms underlying the effects of bryostatin 1 in MCF-7-PKC-α cells have yet to be elucidated. In certain cell types, the dose-dependent responses of bryostatin 1 and the dominant effects of this agent over TPA have been correlated with more pronounced downregulation of a specific PKC isoform by bryostatin that is believed to be required to elicit the cellular response (27, 28). In other cells, the biphasic cellular response of bryostatin 1 correlates with depletion of a specific PKC isoform at low concentrations of this agent and abrogation of downregulation of the same isoform in cells treated with higher doses of bryostatin 1 (32, 33). Regardless of the mechanism responsible for the concentration-dependent effects of bryostatin 1 in MCF-7-PKC-α cells, these results demonstrate that bryostatin 1 may exert varying degrees of antineoplastic efficacy toward specific forms or classes of breast neoplasias. Given that MCF-7-PKC-α cells were generated by overexpression of PKC-α and have multiple alterations in endogenous PKC isoform expression, it is possible that alterations in the PKC pathway were essential for inducing and maintaining the more transformed phenotype exhibited by MCF-7-PKC-α cells. By downregulating the isoform(s) maintaining viability of MCF-7-PKC-α cells, TPA and low doses of bryostatin 1 could interrupt the signal transduction required for MCF-7-PKC-α cell viability and could induce cell death. Thus, utilization of the PKC pathway to maintain viability of the MCF-7-PKC-α cell could render this cell preferentially susceptible to cytotoxic responses elicited by bryostatin 1 and phorbol esters. Therefore, differences in the clinical efficacy of bryostatin 1 among various neoplasias and even within a specific form of neoplasia, such as breast cancer, could be a function of the specific mechanisms used by the neoplasia to subvert normal growth control and to undergo malignant transformation.

These studies suggested that *gadd45* may be involved in the signal cascade leading to death of MCF-7-PKC-α cells. TPA induction of *gadd45* preceded the onset of MCF-7-PKC-α cell death. Nuclear run-on studies demonstrated an enhanced basal level of *gadd45* transcription in MCF-7-PKC-α cells that was further increased within a 30-min exposure to TPA. The ability of cycloheximide to block TPA-stimulated expression of *gadd45* demonstrated a requirement for ongoing protein synthesis to mediate TPA-induced increases in the levels of this gene. The mechanisms underlying the transcriptional activation of *gadd45* in MCF-7-PKC-α cells have not yet been delineated. Phorbol ester–induced expression of *gadd45* mRNA transcripts has not been observed in other cell types (49). Thus, it was somewhat surprising to observe the robust, immediate response of this gene to TPA treatment in MCF-7-PKC-α cells. A p53 response element is contained in the *gadd45* gene and its expression is positively regulated by this transcription factor (47). However, TPA induction of *gadd45* in MCF-7-PKC-α cells occurred in the absence of detectable p53 levels or functional p53-mediated transcriptional activity. An AP-1 site located in the third intron near the p53 site is also present in the *gadd45* gene (47). However, a role for AP-1–mediated induction of this gene has not been demonstrated. In addition to implicating a role for *gadd45* in mediating death of TPA-treated MCF-7-

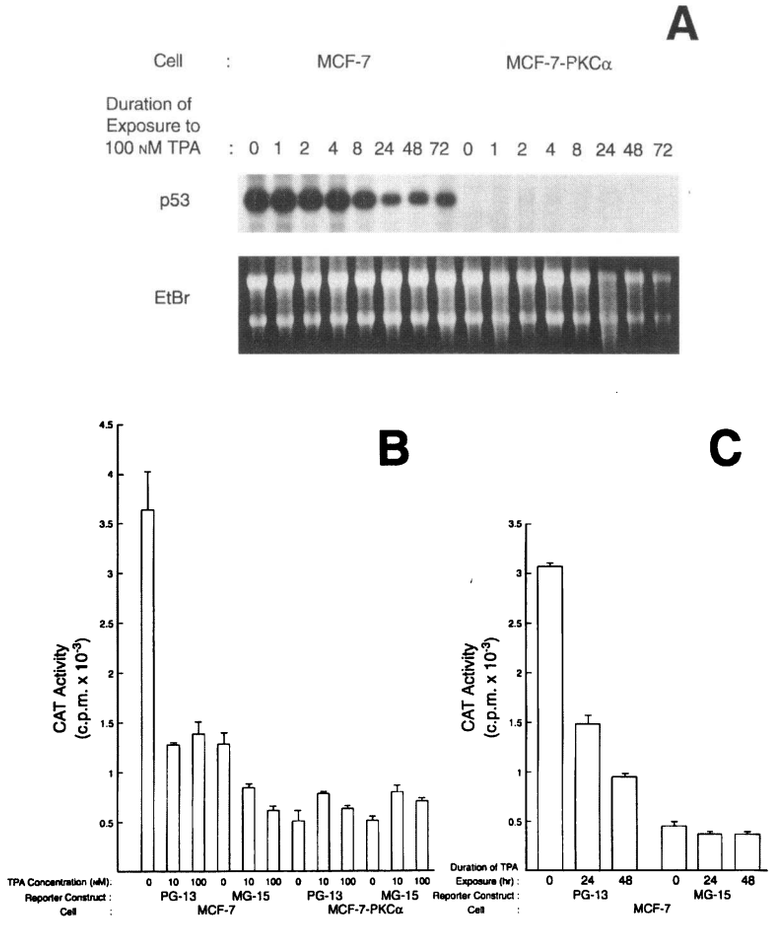

Figure 13. TPA-induced effects on p53 mRNA content and activity in MCF-7 and MCF-7-PKC-α cells. Northern blot analysis of MCF-7 and MCF-7-PKC-α cells treated with 100 nM TPA for varying times (see above the autoradiograms) is shown in *A*. Ethidium bromide staining of the gel is shown beneath the autoradiogram. In *B* and *C*, MCF-7 and MCF-7-PKC-α cells were transiently transfected with either the p53-responsive PG-13-CAT or the mutated, non-p53-responsive MG-15-CAT reporters and treated with different TPA concentrations for 48 h (*B*) or with 100 nM TPA for different times (*C*). CAT activity, shown on the ordinate, was normalized to β-galactosidase levels. Transfections were done in triplicate and were repeated in separate experiments.

PKC-α cells, these findings demonstrate the existence of a phorbol ester–activated, p53-independent pathway that can regulate expression of this gene.

While MCF-7 cells contained readily measurable amounts of p53 mRNA transcripts and protein, this transcriptional factor was not detected in MCF-7-PKC-α cells. Southern blot analysis did not identify a gross gene rearrangement that could account for the absence of p53. Transient transfection analysis using the p53 promoter–CAT construct demonstrated an almost complete lack of transcriptional activation of this promoter in MCF-7-PKC-α cells relative to the levels detected in MCF-7 cells. Thus, the decline of p53 in MCF-7-PKC-α cells was mediated, in part, by decreases in the transcriptional activation of this gene. Given the predominance of other well described mechanisms that inhibit p53 function in human tumors, the significance of whether a decrease in the transcription of this gene as a clinically important phenomenon in human neoplasia remains uncertain. However, these findings do suggest an interaction between the PKC pathway and p53 transcriptional regulation. Lending further support for such an interaction was the ability of TPA to downregulate p53 mRNA transcripts with a concomitant decrease in p53 functional activity as assessed by the transient transfection studies with the PG-13 CAT reporter in MCF-7 cells. A similar TPA-induced decrease in p53 mRNA transcripts has been noted in HeLa and A549 cells (50).

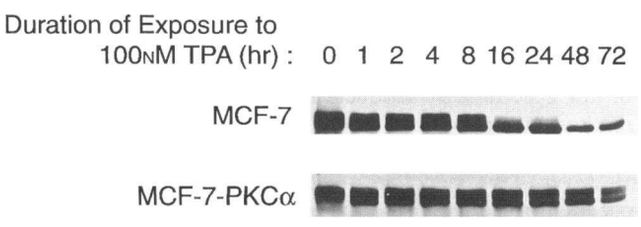

Figure 14. Rb phosphorylation in TPA-treated MCF-7 and MCF-7-PKC-α cells. Western blot analysis using Rb antiserum was done on MCF-7 and MCF-7-PKC-α cells treated with 100 nM TPA for varying times (see above the autoradiogram). Vector-transfected cells yielded similar results to those obtained with MCF-7 cells.

In MCF-7 cells, TPA treatment rapidly stimulated increases in expression of Cip1. The functional significance of induction of this cyclin-dependent kinase interacting protein was apparent in the hypophosphorylated state of Rb and the accumulation of MCF-7 cells in G_1. Transcriptional activation of Cip1 can occur via a p53-dependent mechanism (39–41). Recently, p53-independent modes of inducing Cip1 expression have been described (51–53). Our findings provide evidence to suggest that while MCF-7 cells contain p53, activation of the transcriptional activity of this protein may not be responsible for mediating TPA-induced Cip1 expression. After TPA treatment, p53 mRNA levels declined. In addition, we were unable to detect functional evidence demonstrating an increase in p53-dependent transcriptional activity using transient transfectional analysis with the p53-responsive PG-13-CAT reporter. Furthermore, TPA did not induce the same degree of increase in another

p53-responsive gene, *gadd45,* in MCF-7 cells. Thus, these data suggest that TPA-induced expression of Cip1 in MCF-7 cells may occur by a p53-independent mechanism. The ability of PKC-directed signal transduction to stimulate certain aspects of p53-dependent gene expression would provide a novel means of altering p53-dependent gene transcription in the absence of a functional p53 molecule. A better understanding of the mechanisms by which the PKC pathway can elicit these responses could yield important findings on which to base the design of therapeutic modalities to treat p53-negative neoplasms that are resistant to radiation and certain forms of chemotherapy.

Acknowledgments

The authors wish to express their thanks to June Long for her preparation of this manuscript, Poqiu Gu for her expert assistance in preparing plasmids, the Center for Medical Communications for their preparation of figures and Dr. Pal Bauer for his thoughtful discussions. We appreciate the generosity of Drs. Albert Fornace, Jr. (National Cancer Institute), Steven Elledge (Baylor College of Medicine), and Bert Vogelstein (Johns Hopkins University School of Medicine) in sharing the cDNA plasmids used in this study. We also thank Dr. Marilyn Sleigh (Commonwealth Scientific and Industrial Research Organization, Sydney, Australia) for the gift of the $pSV_2M(2)6$ vector.

This work was partially supported by a grant from the National Institutes of Health (CA-43823).

References

1. Hug, H., and T. Sarre. 1993. Protein kinase C isoenzymes: divergence in signal transduction? *Biochem. J.* 291:329–343.

2. Dekker, L., and P. Parker. 1994. Protein kinase-C a question of specificity. *Trends Biochem. Sci.* 19:73–77.

3. McConkey, D., P. Hartzell, M. Jondal, and S. Orrenius. 1989. Inhibition of DNA fragmentation in thymocytes and isolated thymocyte nuclei by agents that stimulate protein kinase C. *J. Biol. Chem.* 264:13399–13402.

4. Araki, S., Y. Simada, K. Kaji, and H. Hayashi. 1990. Role of protein kinase C in the inhibition of fibroblast growth factor of apoptosis in serum-depleted endothelial cells. *Biochem. Biophys. Res. Commun.* 172:1081–1085.

5. Forbes, I., P. Zalewski, C. Giannakis, and P. Cowled. 1992. Induction of apoptosis in chronic lymphocytic leukemia cells and its prevention by phorbol ester. *Exp. Cell Res.* 198:367–372.

6. Pommier, Y., and N. Colburn. 1992. Acquisition of a growth-inhibitory response to phorbol ester involves DNA damage. *Cancer Res.* 52:1907–1915.

7. Ishi, H., and G. Gobe. 1993. Epstein-Barr virus infection is associated with increased apoptosis in untreated and phorbol ester-treated human Burkett's lymphoma (AW-Ramos) cells. *Biochem. Biophys. Res. Commun.* 192:1415–1423.

8. O'Brian, C., V. Vogel, S. Singletary, and E. Ward. 1989. Elevated protein kinase C expression in human breast tumor biopsies relative to normal breast tissue. *Cancer Res.* 49:3215–3217.

9. Borner, C., R. Wyss, R. Regazzi, U. Eppenberger, and D. Fabbro. 1987. Immunological quantitation of phospholipid/Ca^{2+}-dependent protein kinase of human mammary carcinoma cells: inverse relationships to estrogen receptors. *Int. J. Cancer.* 40:344–348.

10. Lee, S., J. Karaszkiewicz, and W. Anderson. 1992. Elevated level of nuclear protein kinase C in multidrug-resistant MCF-7 human breast carcinoma cells. *Cancer Res.* 52:3750–3759.

11. Fabbro, D., R. Regazzi, S. Costa, C. Borner, and U. Eppenberger. 1986. Protein kinase C desensitization by phorbol esters and its impact on growth of human breast cancer cells. *Biochem. Biophys. Res. Commun.* 135:65–73.

12. Issandou, M., F. Bayard, and J. Darbon. 1988. Inhibition of MCF-7 cell growth by 12-0-tetradecanoylphorbol-13-acetate and 1,2 dioctanoyl-*SN*-glycerol: distinct effects on protein kinase C activity. *Cancer Res.* 48:6943–6950.

13. Kennedy, M., L. Presligiacoma, G. Tyler, W. May, and N. Davidson. 1992. Differentiation effects of bryostatin 1 and phorbol ester on human breast cancer cell lines. *Cancer Res.* 52:1278–1283.

14. Valette, A., N. Gas, F. Roubinet, M. Dupont, and F. Bayard. 1987. Influence of 12-0-tetradecanoylphorbol-13-acetate on proliferation and maturation of human breast carcinoma cells (MCF-7): relationship to cell cycle events. *Cancer Res.* 47:1615–1620.

15. Seynaeve, C., M. Stetler-Stevenson, S. Sebers, G. Kaur, E. Sausville, and P. Worland. 1993. Cell cycle arrest and growth inhibition by the protein kinase antagonist UNC-01 in human breast carcinoma cells. *Cancer Res.* 53:2081–2086.

16. Ways, D., C. Kukoly, J. deVente, J. Hooker, W. Bryant, K. Posekany, D. Fletcher, P. Cook, and P. Parker. 1995. MCF-7 breast cancer cells transfected with protein kinase C-α exhibit altered expression of other protein kinase C isoforms and display a more aggressive neoplastic phenotype. *J. Clin. Invest.* 95:1906–1915.

17. McNeall, J., A. Sanchez, P. Gray, C. Chesterman, and M. Sleigh. 1989. Hyperinducible gene expression from a metallothionein promoter containing additional metal-responsive elements. *Gene (Amst.).* 78:81–88.

18. Pettit, G., C. Herald, D. Doubek, E. Arnold, and J. Calrdy. 1982. Antineoplastic agents 86. Isolation and structure of bryostatin 1. *J. Am. Chem. Soc.* 104:6846–6848.

19. Nicoletti, I., G. Migliorati, M. Pagliancci, F. Grignani, and C. Riccardi. 1991. A rapid and simple method for measuring thymocyte apoptosis by propidium iodide staining and flow cytometry. *J. Immunol. Methods.* 139:271–279.

20. deVente J., S. Kiley, T. Garris, W. Bryant, J. Hooker, K. Posekany, P. Parker, P. Cook, D. Fletcher, and D. Ways. 1995. Phorbol ester treatment of U937 cells with altered protein kinase C content and distribution induces cell death rather than differentiation *Cell Growth & Differ.* 6:371–382.

21. Ways, D., W. Qin, T. Garris, J. Chen, E. Hao, D. Cooper, S. Usala, P. Parker, and P. Cook. 1994. Effects of chronic phorbol ester treatment on protein kinase C activity, content, and gene expression in the human monoblastoid U397 cell. *Cell Growth & Differ.* 5:161–169.

22. Wu, H., and G. Lozano. 1994. NF-κB activation of p53. *J. Biol. Chem.* 169:1–8.

23. White, M., J. deVente, P. Robbins, D. Canupp, M. Mayo, L. Steelman, and J. McCubrey. 1994. Differential regulation of glucose transporter expression in hematopoietic cells by oncogenic transformation and cytokine stimulation. *Oncology Reports.* 1:17–26.

24. Darzynkiewicz, Z., S. Bruno, G. Del Bino, W. Gorczyca, M. Hotz, P. Lassota, and R. Traganos. 1992. Features of apoptotic cells measured by flow cytometry. *Cytometry.* 13:795–808.

25. Prendiville, J., D. Crowther, N. Thatcher, P. Woll, B. Fox, A. McGowan, N. Testa, P. Stern, R. McDermott, M. Potter, and G. Pettit. 1993. A phase one study of intravenous bryostatin 1 in patients with advanced cancer. *Br. J. Cancer.* 68:418–425.

26. Philip, P., D. Rea, P. Thavasu, J. Carmichael, N. Stuart, H. Rockett, D. Talbot, T. Ganesan, G. Pettit, F. Balkwill, and A. Harris. 1993. Phase I study of bryostatin 1: assessment of interleukin 6 and tumor necrosis factor α induction in vitro. *J. Natl. Cancer Inst. (Bethesda).* 85:1812–1818.

27. Blumberg, P. M., and G. R. Pettit. 1992. The bryostatins, a family of protein kinase C activators with therapeutic potential. *In* New Leads and Targets in Drug Research. P. Krogsgaard-Larsen, P. Brogger, S. Christensen, and H. Kofod, editors. Munksgaard International Publishers Ltd., Copenhagen. 273–285.

28. Isakov, N., D. Galron, T. Mustelin, G. Pettit, and A. Altman. 1993. Inhibition of phorbol ester-induced T cell proliferation is associated with rapid degradation of protein kinase C. *J. Immunol.* 150:1195–1204.

29. Hennings, H., P. Blumberg, G. Pettit, C. Harald, R. Shores, and S. Yuspa. 1987. Bryostatin 1, an activator of protein kinase C, inhibits tumor promotion by phorbol esters in SENCAR mouse skin. *Carcinogenesis (Lond.).* 8:1343–1346.

30. Dale, I., and A. Gescher. 1989. Effects of activators of protein kinase C, including bryostatins 1 and 2, on the growth of A549. *Int. J. Cancer.* 43:158–163.

31. Kraft, A., J. Reeves, and C. Ashendel. 1988. Differing modulation of protein kinase C by bryostatin 1 and phorbol esters in JB6 mouse epidermal cells. *J. Biol. Chem.* 263:8437–8442.

32. Szallasi, Z., C. Smith, G. Pettit, and P. Blumberg. 1994. Differential regulation of protein kinase C isozymes by bryostatin 1 and phorbol 12-myristate 13-acetate in NIH 3T3 fibroblasts. *J. Biol. Chem.* 269:2118–2124.

33. Szallasi, Z., M. Denning, C. Smith, A. Dlugosz, S. Yuspa, G. Pettit, and P. Blumberg. 1994. Bryostatin 1 protects protein kinase C-δ from down-regulation in mouse keratinocytes in parallel with its inhibition of phorbol ester-induced differentiation. *Mol. Pharmacol.* 46:840–850.

34. Wyllie, A., J. Kerr, and A. Currie. 1980. Cell death: the significance of apoptosis. *Int. Rev. Cyto.* 68:251–306.

35. Oberhammer, F., J. Wilson, C. Dive, I. Morris, J. Hickman, A. Wakeling, R. Walter, and M. Sikorska. 1993. Apoptotic death in epithelial cells: cleavage of DNA to 300 and/or 50 Kb fragments prior to or in the absence of internucleosomal fragmentation. *EMBO (Eur. Mol. Biol. Organ.) J.* 12:3679–3684.

36. Lowe, S., E. Schmitt, S. Smith, B. Osborne, and T. Jacks. 1993. p53 is required for radiation-induced apoptosis in mouse thymocytes. *Nature (Lond.).* 362:847–849.

37. Clarke, A., C. Purdie, D. Harrison, R. Morris, C. Bird, M. Hooper, and A. Wyllie. 1993. Thymocyte apoptosis induced by p53-dependent and independent pathways. *Nature (Lond.).* 62:849–852.

38. Kastan, M., O. Onyekwere, D. Sidransky, B. Vogelstein, and R. Craig. 1991. Participation of p53 protein in the cellular response to DNA damage. *Cancer Res.* 51:6304–6311.

39. Harper J., G. Adami, N. Wer, K. Keyomarsi, and S. Elledge. 1993. The

p21 CdK-interacting protein Cip1 is a potent inhibitor of G1 cyclin-dependent kinases. *Cell.* 75:805–816.

40. El-Deiry, W., T. Tokino, V. Velculescu, D. Levy, R. Parsons, J. Trent, D. Lin, W. Mercer, K. Kinzler, and B. Vogelstein. 1993. WAF1, a potential mediator of p53 tumor suppression. *Cell.* 75:817–825.

41. El-Diery, W., J. Harper, P. O'Connor, V. Velculescu, C. Canman, J. Jackman, J. Pietenpol, M. Burrell, D. Hill, W. Wang, et al. 1994. WAF1/Cip1 is induced in p53-mediated G1 arrest and apoptosis. *Cancer Res.* 54:1169–1174.

42. Zhan, Q., K. Lord, I. Alamo, Jr., M. Hollander, F. Carrier, D. Ron, K. Kohn, B. Hoffman, D. A. Liebermann, and A. Fornace, Jr. 1994. The *gadd* and *MyD* genes define a novel set of mammalian genes encoding acidic proteins that synergistically suppress cell growth. *Mol. Cell. Biol.* 14:2361–2371.

43. Fornace, A. J., Jr. 1992. Mammalian genes induced by radiation: activation of genes associated with growth control. *Annu. Rev. Genet.* 26:507–526.

44. Fornace, A. J., Jr., J. Jackman, M. C. Hollander, B. Hoffman-Liebermann, and D. A. Liebermann. 1992. Genotoxic-stress-response genes and growth-arrest genes: *Gadd, Myd,* and other genes induced by treatments eliciting growth arrest. *Ann. NY Acad. Sci.* 663:139–153.

45. Hoffman, B., and D. A. Liebermann. 1994. Molecular controls of apoptosis: differentiation/growth arrest primary response genes, proto-oncogenes, and tumor suppressor genes as positive and negative modulators. *Oncogene.* 9:1807–1812.

46. Kastan, M., Q. Zhan, W. El-Deiry, R. Carrier, T. Jacks, W. Walsh, B. Plunkett, B. Vogelstein, and A. Fornace. 1992. A mammalian cell cycle checkpoint pathway utilizing p53 and *gadd45* is defective in ataxia-telangiectasia. *Cell.* 71:578–587.

47. Hollander, M., I. Alamo, J. Jackman, M. Wang, O. McBride, and A. Fornace, Jr. 1993. Analysis of the mammalian *gadd45* gene and its response to DNA damage. *J. Biol. Chem.* 268:24385–24393.

48. Mihara, K., X. Cao, A. Yen, S. Chandler, B. Driscoll, A. Murphel, A. T'Ang, and Y. Fung. 1989. Cell cycle-dependent regulation of phosphorylation of the human retinoblastoma gene produce. *Science (Wash. DC).* 246:1300–1303.

49. Papathanasiou, M., N. Kerr, J. Robbins, O. McBride, I. Alamo, S. Barrett, I. Hickson, and A. Fornace. 1991. Induction by ionizing radiation of the *gadd45* gene in cultured human cells: lack of modulation by protein kinase C. *Mol. Cell. Biol.* 11:1009–1016.

50. Skouv, J., P. Jensen, J. Forchhammer, J. Larsen, and L. Lund. 1994. Tumor-promoting phorbol ester transiently down-modulates the p53 level and blocks the cell cycle. *Cell Growth & Differ.* 5:329–340.

51. Steinman, R., B. Hoffman, A. Iro, C. Guillouf, D. A. Liebermann, and M. El-Houseini. 1994. Induction of p21 (WAF-1/Cip1) during differentiation. *Oncogene.* 9:3389–3396.

52. Michreli, P., M. Chedid, D. Lin, J. Pierce, W. Mercer, and D. Givol. 1994. Induction of WAF1/Cip1 by a p-53 independent pathway. *Cancer Res.* 54:3391–3395.

53. Jiang, H., J. Lin, S. Zao-Zhang, F. Collart, E. Huberman, and P. Fisher. 1994. Induction of differentiation in human promyelocytic HL-60 leukemic cell activates p21, WAF1/Cip1, expression in the absence of p53. *Oncogene.* 9:3397–3405.